# $L$-shell ionizations of Au, Bi, and U in proton and helium-ion impact

H. Tawara
*Nuclear Engineering Department, Kyushu University, Fukuoka, Japan*

K. Ishii and S. Morita
*Department of Physics, Tohoku University, Sendai, Japan*

H. Kaji and T. Shiokawa
*Department of Chemistry, Tohoku University, Sendai, Japan*

(Received 4 September 1974)

The x-ray production cross sections of the total $L$ shell and of the $L\alpha$, $L\beta$, $L\gamma$, $Ll$, and $L\eta$ transitions have been measured for Au, Bi, and U for proton impact over the energy range from 1.0 to 4.5 MeV and for $^3He^+$ impact from 3.0 to 9.0 MeV. The measured x-ray production cross sections and the ratios of the x-ray production for various transitions are compared with calculations based on the plane-wave Born approximation (PWBA) and the binary-encounter approximation (BEA). Generally, the PWBA is in better agreement with the observed results. Various correction factors to these simplified theories are also estimated and discussed. The ratios of the x-ray production for proton impact to that for helium-ion impact, at equal velocities, deviate systematically from the theoretical $Z_1^2$ dependence. This behavior is discussed in terms of the nuclear repulsion for the projectile, the change in binding energy of the target electrons, and the polarization of electron orbit. It is shown that the observed total $L$-shell ionization cross sections for various elements taken from the present work and other works can be represented by a single smooth curve, which at higher energies is in good agreement with the BEA curve of Garcia derived for the $K$-shell ionization, though the experimental values at lower energies are considerably higher than the theoretical predictions.

## I. INTRODUCTION

In recent years considerable attention has been paid to the study of inner-shell ionizations by ion impact in the MeV energy range. The measured $K$-shell ionization cross sections, which have been most extensively investigated, are found to be reproduced fairly well by the plane-wave Born approximation (PWBA)[1] and the binary-encounter approximation (BEA)[2] and are summarized by Rutledge and Watson.[3]

Presently an intensive effort is being made in measurements of the $L$-shell x rays[4-14] as well as those of the Auger electrons.[15] To compare the $L$-shell x-ray data with the ionization cross sections predicted by the theories, the fluorescence yields, and the Coster-Kronig yields of the $L$ shell are required. However, the measurements of these quantities for the $L$ shell are very limited and, furthermore, there exist large discrepancies among the observed values of these yields. The cases where all these parameters are accurately known are very rare[16] (see Table I). McGuire[17] has recently made a calculation of these yields of the $L$ shell for a wide range of elements, which is in general agreement with available experimental values of some elements.

The total $L$-shell x-ray production cross sections can be determined with proportional counters or scintillation counters whose energy resolutions are typically not better than 20%. If the average fluorescence yields $\bar{\omega}$ are known, the total ionization cross sections can be deduced and compared with the theories. There are, however, a number of closely spaced $L$-shell x-ray lines from various transitions resulting from filling a hole in the $L$ shell. These x-ray lines cannot be resolved into each component even with modern Si(Li) detectors which are typically limited to resolutions exceeding 150 eV. Therefore, the determination of the subshell ionization cross sections from x-ray measurements is rather difficult. A number of authors[8,11-14] measured the $L$-shell x-ray production cross sections of the more intense groups (e.g. $L\alpha$, $L\beta$, and $L\gamma$) which usually consist of many unresolved lines, and of certain well-resolved lines such as $Ll$, $L\eta$ with Si(Li) detectors and compared them, instead of the ionization cross sections, with the theories. Datz *et al.*[9] determined the $2s_{1/2}$, $2p_{1/2}$, and $2p_{3/2}$ subshell ionization cross sections of Au in proton and helium-ion impacts from x-ray measurements by a careful peak separation. Madison *et al.*[10] and Abrath and Gray[11] also made similar measurements by proton impact on Pb and Bi, and on Sm, respectively. These groups have found a structure in the $2s_{1/2}$ subshell ionization cross sections predicted by the PWBA. In the present paper, following our previous studies,[13,14] we present the results of measurements of the $L$-shell x-ray pro-

TABLE I. Fluorescence yields and the Coster-Kronig yields of Au, Bi, and U. The theoretical values are taken from the paper of McGuire and the starred values are extrapolated from his calculation. The experimental values are from the paper of Bambynek *et al*.

| | $\omega_1$ | | $\omega_2$ | | $\omega_3$ | | $f_{12}$ | | $f_{13}$ | | $f_{23}$ | |
|---|---|---|---|---|---|---|---|---|---|---|---|---|
| | Theor. | Expt. | Theor. | Expt. | Theor. | Expt. | Theor. | Expt. | Theor. | Expt. | Theor. | Expt. |
| Au | 0.105 | ••• | 0.357 | ••• | 0.327 | 0.31 | 0.083 | 0.25 | 0.644 | 0.51 | 0.132 | ••• |
| Bi | 0.120 | ••• | 0.417 | ••• | 0.389 | 0.36 | 0.069 | 0.19 | 0.656 | 0.58 | 0.101 | 0.06 |
| U | 0.215* | ••• | 0.560* | ••• | 0.480* | 0.51 | 0.069* | ••• | 0.55* | ••• | 0.23* | 0.23 |

duction cross sections of Au, Bi, and U targets for proton (1.0–4.5 MeV) and $^3He^+$ (3.0–9.0 MeV) impact using a Si(Li) detector and compare these results with the theoretical predictions. Based on these measurements, we discuss the dependence of the $L$-shell ionization cross section on the projectile nuclear charge. The total $L$-shell ionization cross sections of various elements, deduced from x-ray data using the average fluorescence yields, are compared with the BEA universal curve.

## II. EXPERIMENTAL PROCEDURES

The experimental procedures used in the present work are very similar to those reported previously.[13] Only a brief description relevant to the present measurement is given here. The Au and Bi targets were prepared by vacuum evaporation of the respective pure metals onto 100-$\mu g/cm^2$ Al-backing foils. The U target was prepared by electrospraying[18] of a solution of uranylacetate $[(CH_3COO)_2UO_2 \cdot 2H_2O]$ onto the 100-$\mu g/cm^2$ Al foil. The thicknesses of the Au, Bi, and U targets were determined to be 348, 431, and 291 $\mu g/cm^2$, respectively, from the Rutherford scattering of 3.5-MeV protons.

Typical spectra of the $L$-shell x rays produced by proton impact are shown in Fig. 1. Spectra for $^3He^+$ impact are very similar to those in Fig. 1. Assuming that the $L$-shell x-ray production is isotropic, the x-ray production cross section $\sigma_x$ is obtained from the following formula:

$$\sigma_x = (4\pi/\Delta\Omega)(Y/n), \tag{1}$$

where $\Delta\Omega$ is the solid angle subtended by the x-ray detector, $Y$ is the x-ray yield per projectile, corrected for the absorption in the target, a Mylar window, and the air path and for the detection efficiency of the detector, and $n$ is the number of target atoms per $cm^2$. The estimated errors are about 15% for the $L\alpha$, $L\beta$, and $L\gamma$ x-ray groups, 17% for the $Ll$ x rays for all targets, about 35% for the $L\eta$ x rays of Bi and Au, and 50% for those of U.

## III. EXPERIMENTAL RESULTS AND DISCUSSIONS

### A. Proton impact

#### *1. Partial x-ray production cross sections for La, Lβ, Lγ, Ll, and Lη transitions*

In x-ray measurements like the present one, the x-ray lines in the $L\alpha$, $L\beta$, and $L\gamma$ groups cannot be resolved because of the limited energy resolution of the x-ray detector. The partial x-ray production cross sections for these transitions can be calculated by the following formulas[13]:

$$\sigma_x^{L\alpha} = [\sigma_i^{L1}(f_{13} + f_{12}f_{23}) + \sigma_i^{L2}f_{23} + \sigma_i^{L3}]\omega_3(\Gamma_{3\alpha}/\Gamma_3), \tag{2}$$

$$\sigma_x^{L\beta} = [\sigma_i^{L1}(f_{13} + f_{12}f_{23}) + \sigma_i^{L2}f_{23} + \sigma_i^{L3}]\omega_3(\Gamma_{3\beta}/\Gamma_3) + (\sigma_i^{L1}f_{12} + \sigma_i^{L2})\omega_2(\Gamma_{2\beta}/\Gamma_2) + \sigma_i^{L1}\omega_1(\Gamma_{1\beta}/\Gamma_1), \tag{3}$$

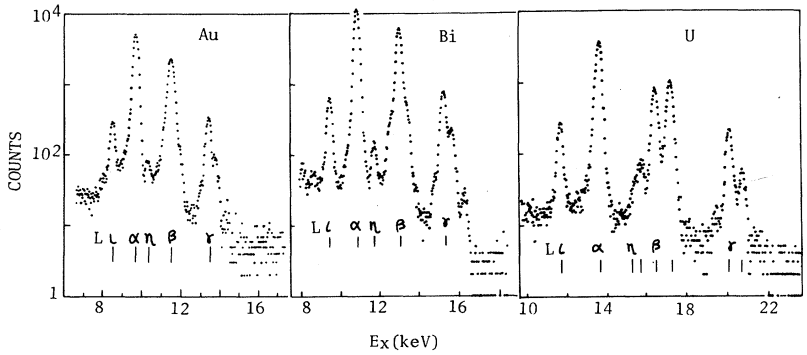


FIG. 1. Typical $L$-shell x-ray spectra from Au, Bi, and U targets for proton impact.

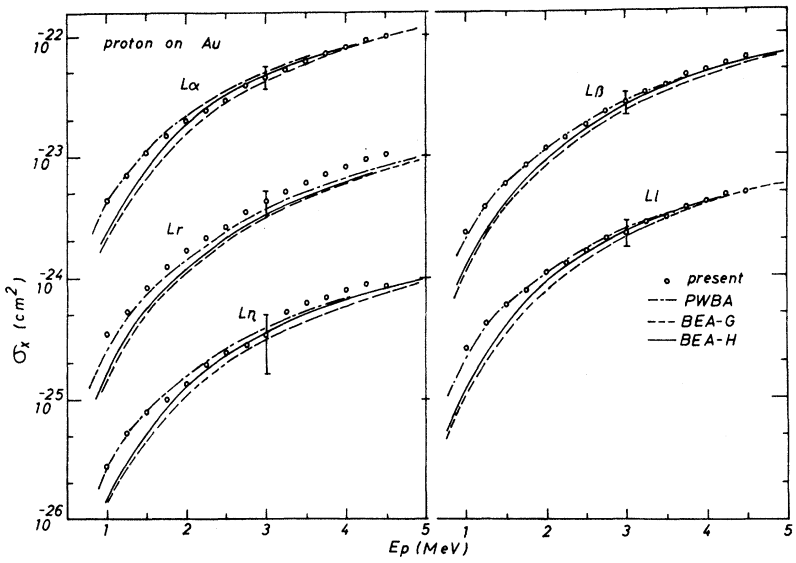


FIG. 2. Partial $L$-shell x-ray production cross sections for Au with proton impact. The curves labeled PWBA, BEA-G, and BEA-H are based on the PWBA of Choi *et al.*, the BEA of Garcia, and the BEA of Hansen. Typical errors are shown with bars.

$$\sigma_x^{L\gamma} = (\sigma_i^{L1} f_{12} + \sigma_i^{L2})\omega_2(\Gamma_{2\gamma}/\Gamma_2) + \sigma_i^{L1}\omega_1(\Gamma_{1\gamma}/\Gamma_1), \tag{4}$$

$$\sigma_x^{Ll} = [\sigma_i^{L1}(f_{13} + f_{12}f_{23}) + \sigma_i^{L2}f_{23} + \sigma_i^{L3}]\omega_3(\Gamma_{3l}/\Gamma_3), \tag{5}$$

$$\sigma_x^{L\eta} = (\sigma_i^{L1} f_{12} + \sigma_i^{L2})\omega_2(\Gamma_{2\eta}/\Gamma_2). \tag{6}$$

Here $f$ and $\omega$ are the Coster-Kronig yield and the fluorescence yield, respectively; $\Gamma$ is the theoretical radiative transition rate calculated by Scofield[19]; and $\sigma_i^{Lj}$ is the ionization cross section of the $j$th subshell and can be calculated from the PWBA or the BEA. All values of $f$ and $\omega$ are not always accurately known and, therefore, we use the calculated values of McGuire[17] (see Table I).

The measured results for Au, Bi, and U targets are shown in Figs. 2, 3, and 4, respectively, and are compared with the theoretical predictions based on the PWBA of Choi *et al.*[20] (labeled as PWBA), the BEA of Garcia[2] (BEA-G), and the BEA of Hansen[21] (BEA-H). Although there are always some uncertainties in the fluorescence yields and Coster-Kronig yields, the measured cross sections are generally better reproduced by the PWBA both in the shape (energy dependence) and the absolute values over the energy range investigated. At lower energies, both of the BEA-G and BEA-H are systematically lower than the experimental data. All the theoretical predictions come close together at higher energies and are in good agreement with the observed results. The present data on Au agree well with those of Akselsson and Johansson.[12]

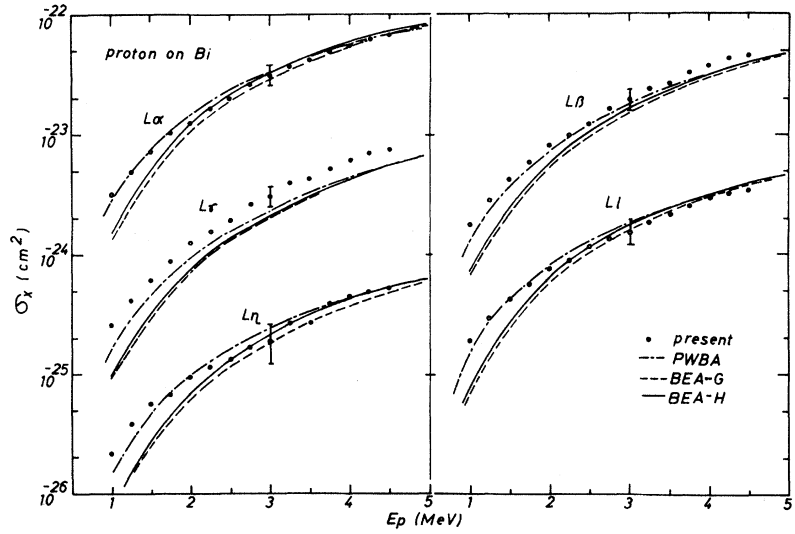


FIG. 3. Partial $L$-shell x-ray production cross sections for Bi with proton impact. The notations are the same as in Fig. 2.

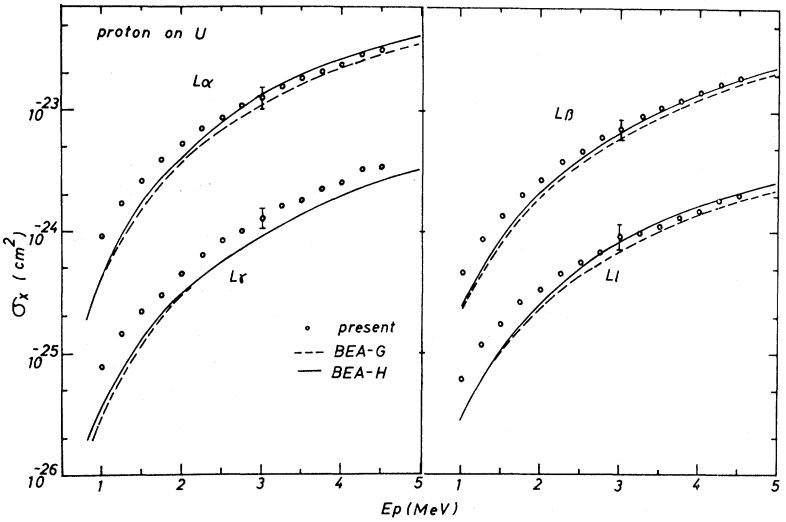


FIG. 4. Partial $L$-shell x-ray production cross sections of U in proton impact. The notations are the same as in Fig. 2.

### 2. *Total L-shell x-ray production cross sections*

The theoretical total $L$-shell x-ray production cross section $\sigma_x^L$ is calculated by the following equation[13]:

$$\sigma_x{}^L = \sum_{j=1}^{3} \omega_j{}^{\text{eff}} \sigma_i{}^{L_j} , \tag{7}$$

where $\omega_j{}^{\text{eff}}$ is the effective fluorescence yield of the $j$th subshell taking into account the Coster-Kronig yield and the fluorescence yield of other subshells. On the other hand, the experimental total $L$-shell x-ray production cross section is given as the sum of cross sections for all the transitions,

$$\sigma_x{}^L = \sigma_x{}^{L\alpha} + \sigma_x{}^{L\beta} + \sigma_x{}^{L\gamma} + \sigma_x{}^{Ll} + \sigma_x{}^{L\eta} . \tag{8}$$

In Figs. 5, 6, and 7 are shown the measured total x-ray production cross sections for Au, Bi, and U targets, together with the theoretical predictions of the PWBA and the BEA. For total cross sections, some other experimental results of Au and U are available for a comparison. Akselsson and Johansson[12] measured the $L$-shell x rays of Au over the energy range from 1.5–11 MeV, which are in good agreement with the present data in the overlapped energy range. But the data of Shafroth *et al.*[6] and of Fahlenius and Jauho[22] are systematically smaller than the present results. In all these measurements, modern Si(Li)

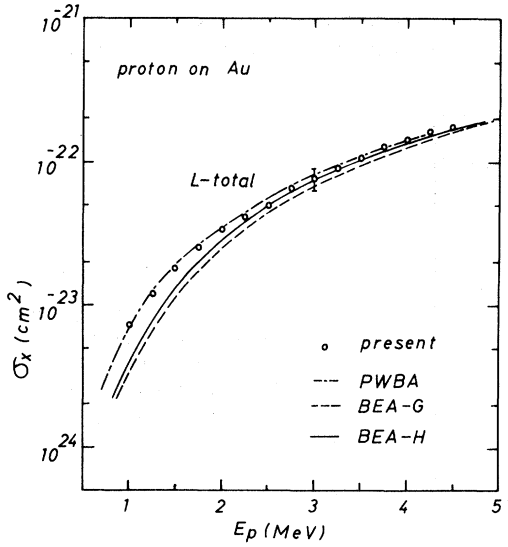


FIG. 5. Total $L$-shell x-ray production cross sections of Au in proton impact. The notations are the same as in Fig. 2.

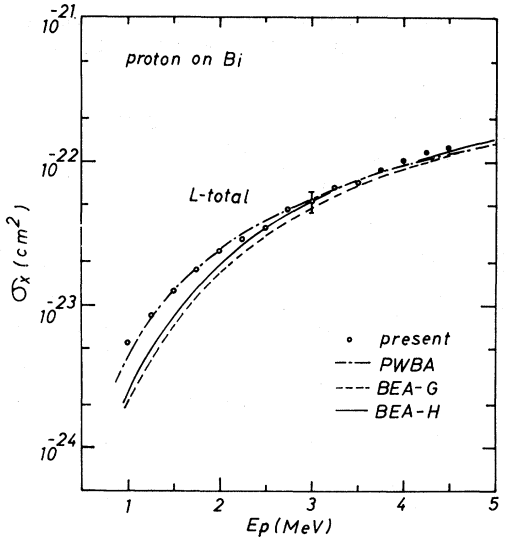


FIG. 6. Total $L$-shell x-ray production cross sections of Bi in proton impact. The notations are the same as in Fig. 2.

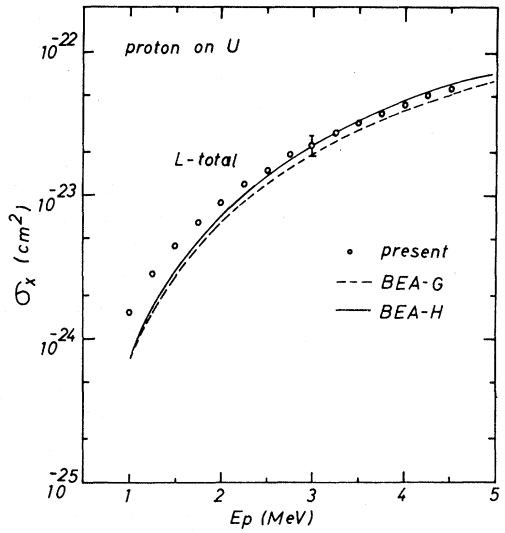


FIG. 7. Total $L$-shell x-ray production cross sections of U in proton impact. The notations are the same as in Fig. 2.

x-ray detectors and thin targets were used. It may be worthy to note that the data of Bernstein and Lewis[23] for Au and U, which were deduced from thick target yields measured with an NaI (Tl) scintillation detector without resolving various components, agree with the present data within (5–10)% uncertainties.

### 3. *Intensity ratios of x-ray production of various groups*

As pointed out in a previous paper,[13] the measured ratios of the x-ray production cross sections, such as $L\alpha/L\beta$, $L\alpha/L\gamma$, provide a rigorous test of the theoretical predictions because a number of experimental uncertainties are cancelled out. The ratios obtained in the present study are shown in Figs. 8, 9, and 10 for Au, Bi, and U targets, respectively, along with the theoretical predictions. Other experimental data are also shown. In Au and Bi data, the shapes of experimental curves are reproduced by the PWBA apart from the absolute values. The BEAs of Garcia and

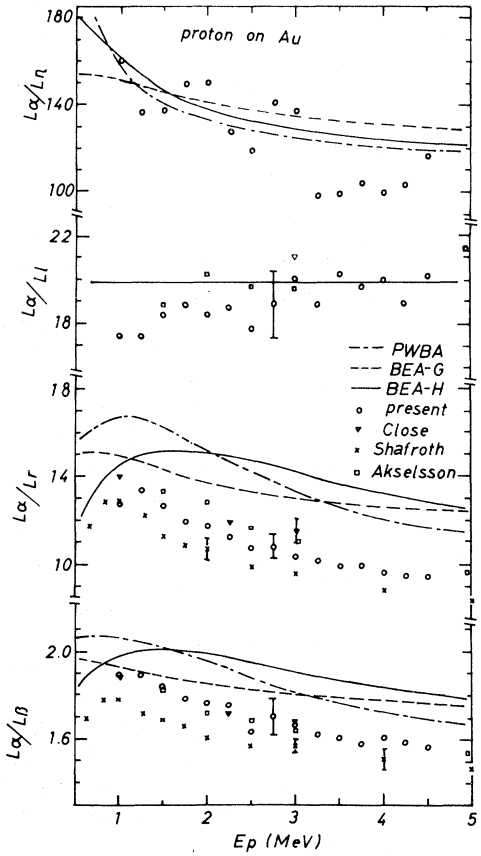


FIG. 8. Ratios of the $L$-shell x-ray intensity in various groups in Au for proton impact. The notations are the same as in Fig. 2.

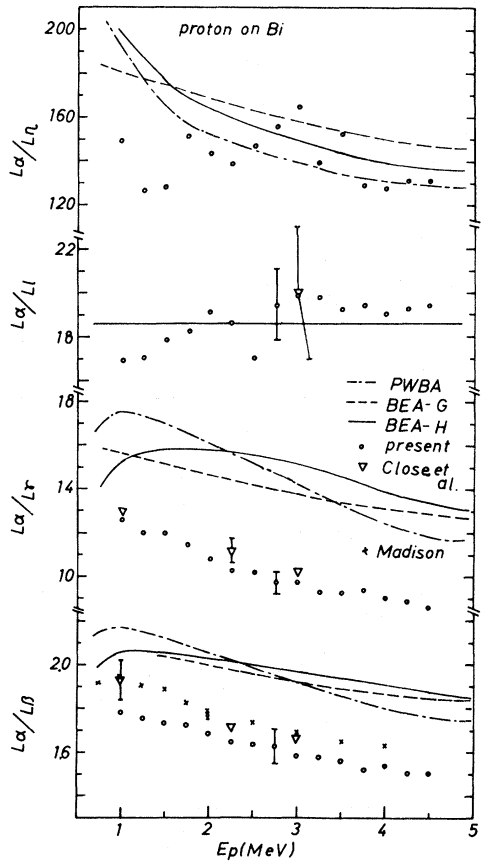


FIG. 9. Ratios of the $L$-shell x-ray intensity in various groups in Bi for proton impact. The notations are the same as in Fig. 2.

of Hansen fail to reproduce the observed results, especially at lower energies. The expected peaks of the BEA of Hansen are broad and the positions appear at much higher energies than the measured results. Most of the experimental values, especially the data of the present study and of Close *et al.*,[24] are in good agreement with each other within error limits, though Au data of Shafroth *et al.*[6] and Bi data of Madison *et al.*[10] deviate systematically from the present results. For U data, the BEA of Garcia reproduces well the measured $L\alpha/L\beta$ ratio, whereas that of Hansen shows a shape different from the measurement. From a theoretical point of view, the $L\alpha/Ll$ ratio should

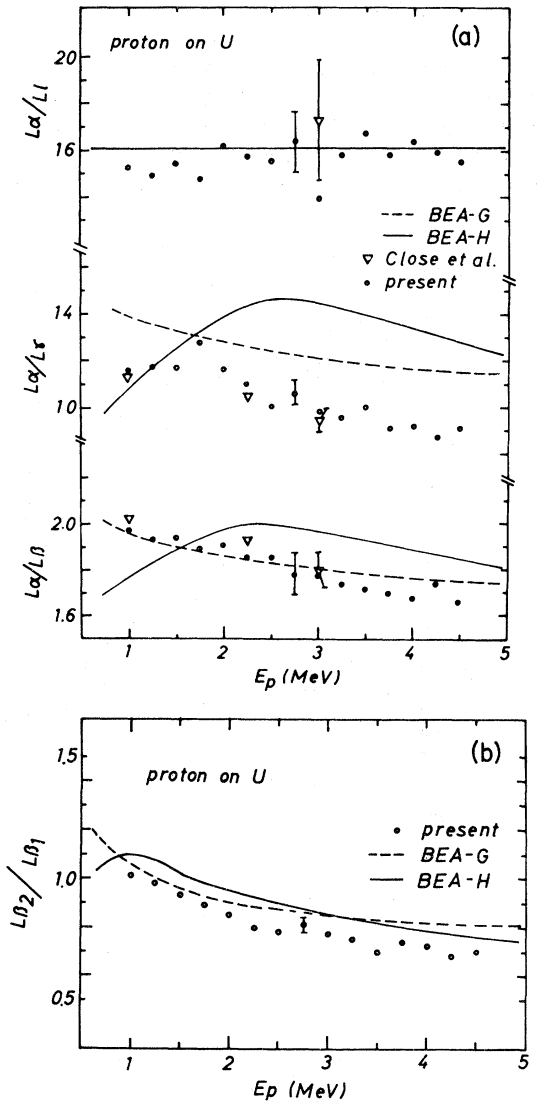


FIG. 10. Ratios of the $L$-shell x-ray intensity in various groups in U for proton impact. The notations are the same as in Fig. 2.

be constant and independent of the energy of the projectile because both x rays arise from the primary vacancies in the $L_3$ subshell. However, both in the present data and those of Akselsson and Johansson,[12] the $L\alpha/Ll$ ratio seems to be slightly dependent on the proton energy, increasing with the increase of the energy in the energy range investigated. This is probably due to the difference in the effect of the simultaneous outer-shell ionization in both transitions. In Table II, a comparison is given of the $L\alpha/Ll$ ratios of the present data with those in other experiments[12,24-28] and the theoretical predictions of Scofield. In this table, the data for proton and helium-ion impact are shown by simply averaged values, neglecting the slight energy dependence. The present data show no significant difference of the $L\alpha/Ll$ ratio in proton and helium-3 ion impact and are in reasonable agreement with the calculation of Scofield.

#### 4. *Various corrections to the theories*

As seen in Figs. 2–7, observed x-ray production cross sections are generally reproduced by both the PWBA and BEA. These theories, simplified in many respects, are based on the straight-line trajectory, constant-velocity approximation using nonrelativistic hydrogenic wave functions for inner-shell electrons. However, especially in the ionization of heavy elements, we have to take into account various corrections to these theories. Now we discuss correction factors.

a. *Relativistic effect.* In heavy elements, inner-shell electrons should be treated using relativistic wave functions. A rigorous relativistic treatment of $L$-shell ionization based on the PWBA has been given by Choi[29] for some elements and compared with experimental data in Au. Hansen[21] also gave the relativistic effect on the $K$-shell ionization based on the BEA. Alternatively, the relativistic ionization cross section in the PWBA can be obtained from the nonrelativistic cross section through a reduction in $\theta$, the screening number. This reduction is equivalent to the reduction of the binding energy, which results in increasing the cross section in the present energy range. The relativistic $\theta$ can be estimated in a way given previously.[1,14] Using equivalent reduction of the binding energy, the relativistic ionization cross section is easily determined from the BEA. By comparing the relativistic cross section with the nonrelativistic cross section, the relativistic correction factor is extracted and, as an example, shown in Fig. 11 for the total $L$ x-ray production cross section in Bi (labeled $R$). This factor is considerably large among correction factors discussed here.

b. *Binding effect.* The binding energy of target

electrons increases due to the proximity of projectile. This binding effect reduces the ionization cross section. Following a method proposed by Brandt and Lapicki,[30] we obtain the binding correction factor as shown in Fig. 11 (labeled *B*). This correction factor is not large.

c. *Deflection effect.* A projectile is deflected away in a Coulomb field of target nucleus and its path is not straight. Thus, the ionization cross section is reduced. A procedure for estimating the deflection effect for the *L* shell was given by Brandt and Lapicki.[30] The deflection correction factor is shown in Fig. 11 (labeled *C*). This correction factor is large at lower energies, decreasing with increasing the impact energy.

d. *Retardation effect.* To estimate the retardation effect, we use a procedure of Garcia[2] who gave a formula for the reduction of kinetic energy of projectile due to the repulsive force from target nucleus. This retardation correction factor is given in Fig. 11 (labeled *r*).

e. *Charge-transfer effect.* Some inner-shell electrons of the target atom can be transferred to orbits of the projectile during collision, resulting in the ionization. The ionization cross section due to electron transfer is estimated using the BEA of Garcia *et al.*[31] It is found that, in these heavy elements, contribution of the charge transfer to *L*-shell ionization is less than 1%. Therefore, the charge-transfer correction factor is small.

f. *Multiple ionization and fluorescence yield.* We estimate probability of simultaneous ionization using a method of McGuire and Richard.[32] It is found that the probability of *L*-shell ionization of Bi, accompanied with one *M*-shell ionization, is at most 3% of pure *L*-shell ionization at 5 MeV, decreasing with decreasing the impact energy. Therefore, the variation of the fluorescence yields due to multiple ionization is estimated to be small, though no theoretical estimations of its variation in *L* shell are available for these heavy elements. Also it should be noted that the fluorescence yields and Coster-Kronig yields used in the present analysis are calculated in the nonrelativistic approximation and, therefore, may not be the same as those in the relativistic approximation which is necessary for heavy elements.

The net correction factor labeled NET is about (10–20)% in the present energy range because some of the correction factors are canceled out with each other. Taking into account uncertainties of the present measurement (~15%), it is concluded that the PWBA and BEA, though oversimplified, can reproduce the observed data due to cancellation of various correction factors.

TABLE II. $L\alpha/Ll$ ratio for Au, Bi, and U.

| | Theory | Experiment | | | |
|---|---|---|---|---|---|
| Au | 19.9 | 18.9±1.5[a] | 17.9±1.4[b] | 21.0±3.2[c] | 20.45[d] |
| Bi | 18.6 | 18.7±1.5[a] | 18.2±1.4[b] | 20.1±3.0[c] | |
| U | 16.1 | 15.6±1.2[a] | 15.9±1.3[b] | 17.3±2.6[c] | 16.1±0.8[e] |
| | | 15.9±1.0[f] | 16.3±0.5[g] | 15.0±1.4[h] | |

[a] Present (1.0–4.5-MeV proton).
[b] Present (3.0–9.0-MeV helium-3).
[c] Close *et al.*, Ref. 24 (3.0-MeV proton).
[d] Akselsson and Johansson, Ref. 12 (1.5–11-MeV proton).
[e] Wyrick and Cahill, Ref. 25 (26-MeV $\alpha$ particle).
[f] Nix *et al.*, Ref. 26 (radioisotope).
[g] Rao *et al.*, Ref. 27 (radioisotope).
[h] McCrary *et al.*, Ref. 28 (x ray).

### B. Helium-3 ion impact

Similar x-ray measurements have been made in helium-3 ion impact on Au, Bi, and U targets over the energy range from 3.0 to 9.0 MeV. The observed results are shown in Fig. 12. As will be described later, the theoretical predictions deviate considerably from the observations in helium-ion impact. Therefore, no attempt has been made to compare the experimental data with the theories. Discussions on the dependence of the *L*-shell x-ray production on the nuclear charge of the projectile will be given in the next section.

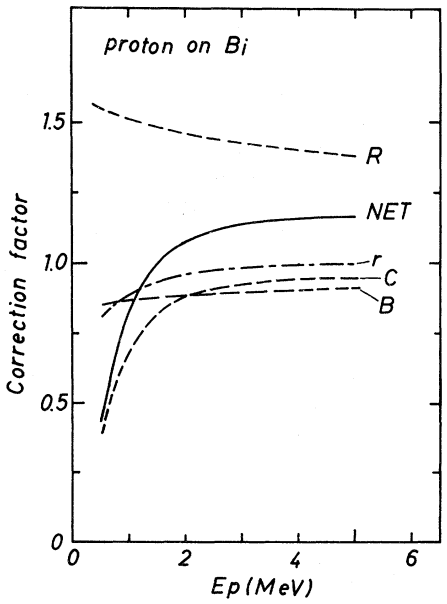


FIG. 11. Various correction factors to the simplified theory for Bi. *R*, the relativistic correction factor; *B*, the binding correction factor; *C*, the deflection correction factor; *r*, the retardation correction factor; NET, the over-all correction factor.

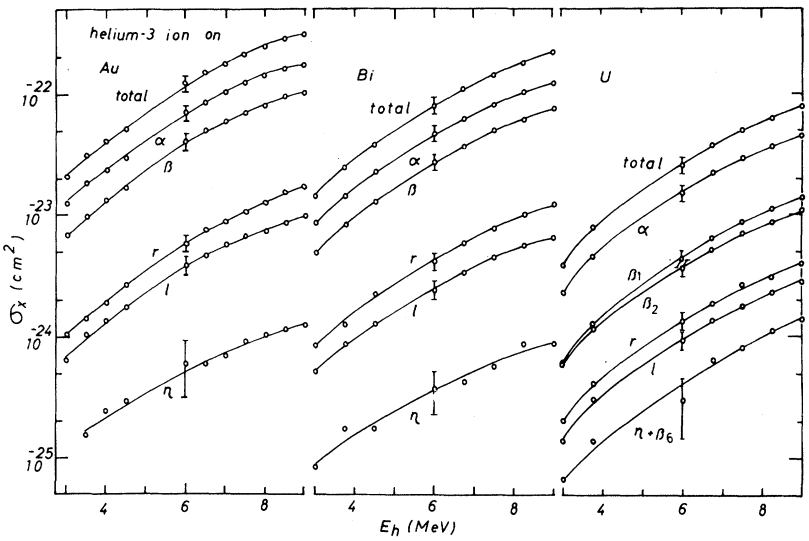


FIG. 12. $L$-shell x-ray production cross sections for Au, Bi, and U targets with $^3He^+$ impact. The solid curves are drawn to guide the eye.

### C. $Z_1$-dependence of the $L$-shell x-ray production

In contrast to the theoretical calculations of the PWBA and the BEA, which predict that the inner-shell ionization cross sections are proportional to the square of the nuclear charge of the projectile $Z_1$, the measured results on the $K$-,[33,34] $L$-,[13] and also $M$-shell[35] ionizations deviate significantly from this prediction, especially at low energies. This deviation in the $K$-shell ionization has been explained by Basbas *et al.*[33] in terms of the Coulomb deflection of the projectile by target nucleus, the increased binding energy of the target electrons due to the proximity of the projectile, and the polarization of the inner-shell orbit. This explanation has been successfully extended to the $L$-shell ionizations by Tawara *et al.*[13] resulting in fairly good agreements with the measured $L$-shell data. According to discussions of Basbas *et al.*[33] and Lewis *et al.*,[34] the ratio, divided by $Z_1^2$, of the ionization cross sections for projectile of nuclear charge $Z_1$ to those for protons at equal velocities, $\sigma(Z_1)/Z_1^2\sigma(\mathrm{H})$, is smaller than unity at low energies and becomes larger than unity at high energies before reaching unity at much higher energies. Thus, the ratio is expected to be unity at an intermediate energy, which we call the crossover point for simplicity. The expected crossover point for the $L$-shell ionization, $E_c$(MeV/amu), is given as follows,[13]

$$E_c = 1.83 U_L (2U_L/\Re Z_L^2)^2 , \qquad (9)$$

where $U_L$ is the binding energy of the shell considered in keV, $\Re$ is the Rydberg constant, and $Z_L$ is the effective nuclear charge of the $L$ shell and is taken as $(Z_2 - 4.15)$, $Z_2$ being the nuclear charge of the target. The crossover points given by Eq. (9) are shown by arrows in Fig. 13, where the experimental ratios of the production cross sections for the $L\alpha$, $Ll$, and total $L$ x rays for proton impact to those for helium-3 ion impact, $\sigma(\mathrm{He})/4\sigma(\mathrm{H})$, are shown as a function of the projectile energy per amu. For the total $L$ x-ray production cross section, the binding energies are taken as the averaged values. Note that the primary vacancies in the $L\alpha$ and $Ll$ transitions are produced only in the $L_3$ subshell. The observed ratios are always much smaller than unity at low energies for Au, Bi, and U targets. The observed crossover points for the $L\alpha$ and $Ll$ x rays are very close to the expected values shown by arrows. From the present results and the previous one[13] on Pb, Eq. (9) is thought to give

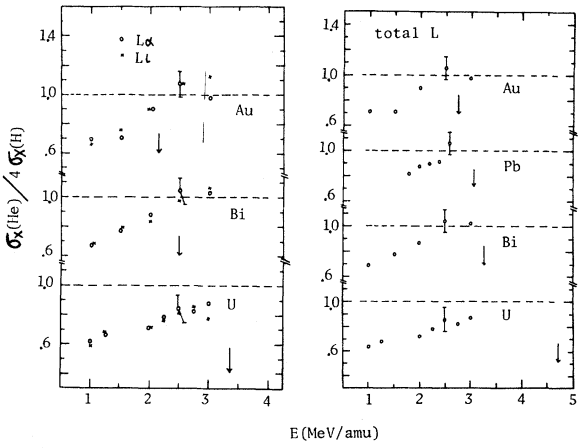


FIG. 13. Ratio of production cross sections of the $L\alpha$, $Ll$, and total $L$ x ray for $^3He^+$ impact to those for proton impact on Au, Bi, and U targets. The arrows show the crossover points predicted from Eq. (9).

a good estimation of the crossover points for the $L$-shell x-ray production ratios in proton and helium-ion impact so far as the $L_3$ subshell is concerned. This can be expected because the energy distribution of the electrons in the $L_3$ subshell is similar to that in the $K$ shell. It should be noted that Eq. (9) is based on that derived for the $K$-shell ionization and modified slightly. As for the total $L$ x-ray production, the observed crossover points are lower than the values calculated from Eq. (9), the discrepancy increasing with the increase in the nuclear charge of the target. At present, there are no exact theoretical explanations for this discrepancy. Possible reason might be the difference in the energy and density distributions of the $L$-shell electrons, especially of the $L_1$-subshell electrons from those of the $K$-shell electrons. The $L_1$ subshell contributes considerably to the total $L$-shell ionization, as shown by Datz *et al.*[9] Furthermore, it is believed that other processes discussed in a previous section, for example, the charge-transfer and multiple-ionization processes,[36,37] in addition to three effects mentioned here, might play a role in the deviation from the $Z_1^2$ dependence. It would be desirable to study the contribution of these processes to the inner-shell ionization theoretically and experimentally.

### D. Universal curves for the $L$-shell ionizations

As expected from the BEA of Garcia, the $K$-shell ionization cross sections by ion impact can be expressed by a single universal curve, when the cross section $\sigma_i^K$ is expressed in the form of $U_K^2\sigma_i^K/Z_1^2$, as a function of $E/U_K$. Here $U_K$ is the binding energy of the $K$-shell electron of the target and $E$ is the energy of the projectile. Hardt and Watson[38] tried to fit the $K$-shell ionization data for a number of elements to a single smoothed curve. It has been found that proton data are still scattered around the BEA curve but their data in $\alpha$-particle impact fit surprisingly well to a single curve, with the relativistic correction to the inner-shell electron velocity, which is slightly lower than the BEA curve. A similar universal curve is also expected in the $L$-shell ionization.

From the measured total $L$-shell x-ray production cross section $\sigma_x^L$, the total $L$-shell ionization cross section $\sigma_i^L$ can be determined by $\sigma_i^L = \sigma_x^L/\tilde{\omega}_L$,

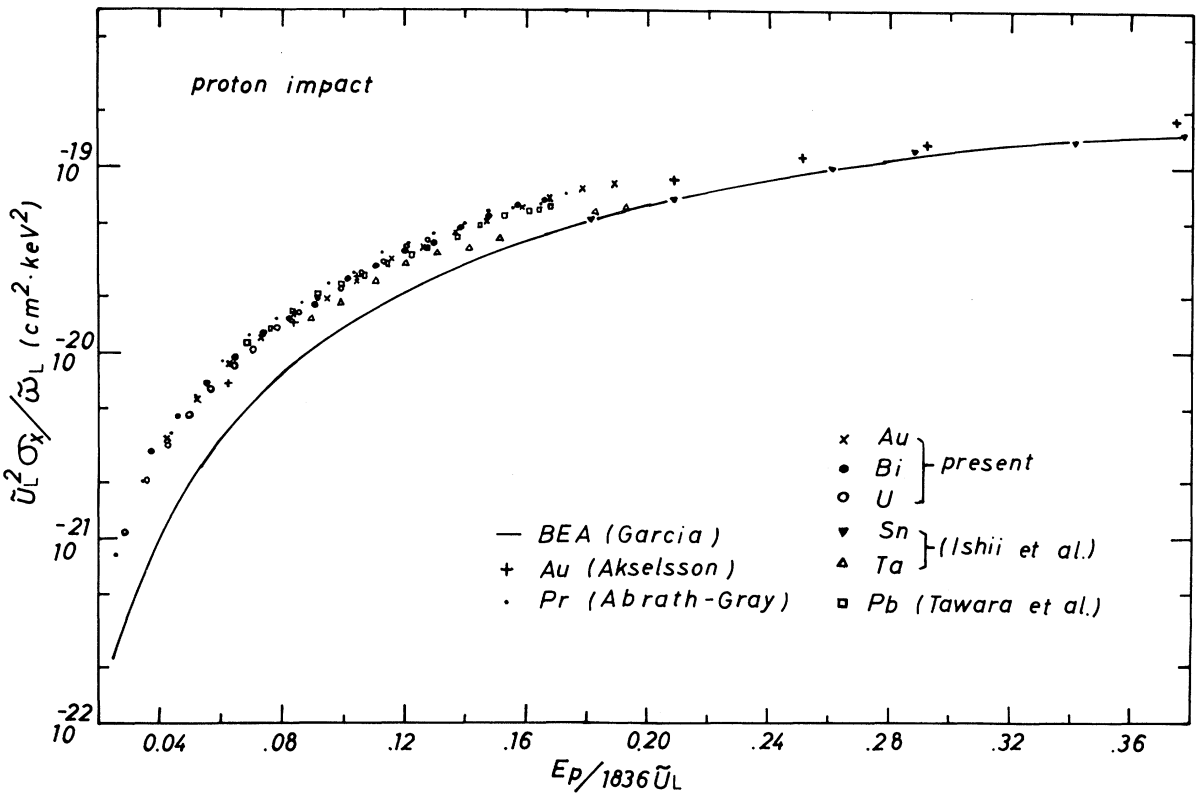


FIG. 14. Total $L$-shell ionization cross sections for proton impact expressed in a universal form. The solid curve shows the BEA prediction of Garcia. The averaged fluorescence yields are 0.09 for Sn, 0.14 for Pr, 0.28 for Ta, 0.35 for Au, 0.38 for Pb, 0.40 for Bi, and 0.52 for U, respectively.

if the average fluorescence yield $\bar{\omega}_L$ is known. However, $\bar{\omega}_L$ is known. However, $\bar{\omega}_L$ is not always measured accurately. Theoretically, $\bar{\omega}_L = \sum_{j=1}^{3} (N_{Lj}/8)\omega_j^{\text{eff}}$, where $N_{Lj}$ is the number of electrons in the $j$th subshell and $\omega_j^{\text{eff}}$ is the effective fluorescence yield discussed in Eq. (7). In Fig. 14 are plotted the values of $\tilde{U}_L^2 \sigma_x^L / \bar{\omega}_L$ for various targets in proton impact, measured in the present work and also in other works, as a function of $E/1836\tilde{U}_L$, together with the BEA curve of Garcia. Here $\bar{\omega}_L$ is estimated from the paper of Bambynek *et al.*[16] and $\tilde{U}_L$ is the averaged binding energy of the $L$-shell electrons determined from $\tilde{U}_L = \frac{1}{8}(2U_{L_1} + 2U_{L_2} + 4U_{L_3})$, $U_{L_1}$, $U_{L_2}$, and $U_{L_3}$ being the binding energies of the $L_1$-, $L_2$-, and $L_3$-subshell electrons, respectively. The BEA curve is systematically lower than the measured data at low energies but the agreement between the BEA and the experiments is good at high energies. Also in Fig. 15 is given a similar plot in helium-3 ion impact, where the ordinate is divided by 4, the square of the nuclear charge of helium ions. The general features in Figs. 13 and 14 are very similar, though they are slightly different at low energies. This is in contrast to that in oxygen-ion impact,[39] which is fairly lower than the BEA curve. Due to simultaneous outer-shell ionization, the averaged fluorescence yields in oxygen-ion impact are expected to be large, whereas the binding energies increase. Therefore, the measured smoothed ionization curve expressed in a form of $\tilde{U}_L^2 \sigma_x^L / \bar{\omega}_L$ would not be much different from their curve of oxygen-ion impact if proper fluorescence yields are used. As seen in Figs. 14 and 15, the smoothed universal curve for the $L$-shell ionizations for various elements can be drawn for each projectile. Once the universal curves are established, we can use the curves to determine the average fluorescence yield of the $L$ shell which has not accurately been known, by measuring the total $L$-shell x-ray production cross sections, possibly even with scintillation counters or proportional counters. A similar procedure was proposed by Garcia[2] for determining the fluorescence yield of the $K$ shell.

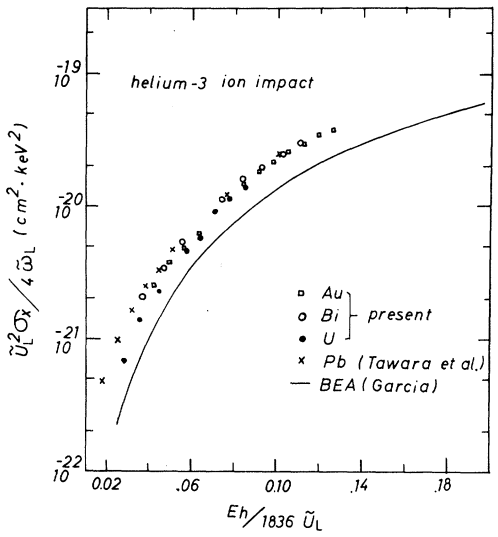


FIG. 15. Total $L$-shell ionization cross sections for $^3He^+$ impact expressed in a universal form. The notations are the same as in Fig. 14.

## IV. CONCLUSIONS

The x-ray production cross sections of the $L\alpha$, $L\beta$, $L\gamma$, $Ll$, and $L\eta$ transitions in Au, Bi, and U have been measured in proton (1.0–4.5 MeV) and helium-3 ion (3.0–9.0 MeV) impacts. The measured x-ray production cross sections are generally better reproduced by the PWBA than by the BEA, when the fluorescence yields and Coster-Kronig yields calculated by McGuire are used. The observed ratios in the $L$-shell x-ray productions in proton impact to those in helium-ion impact $\sigma(\text{He})/4\sigma(\text{H})$ deviate significantly from the theoretical predictions and are much smaller than unity at low energies, approaching unity around the highest energy investigated. The observed crossover points in the $L\alpha$ and $Ll$ x-ray production ratios are in agreement with Eq. (9). However, those in the total $L$-shell x-ray production ratios disagree with the formula. It is pointed out that this discrepancy can be due to the difference of the energy and density distributions of electrons in the $L$ shell from those in the $K$ shell.

It is also shown that the observed total $L$-shell ionization cross sections can be represented in a single smoothed curve which at high energies agrees with the BEA curve of Garcia derived for the $K$-shell ionization.

## ACKNOWLEDGMENT

The authors would like to thank M. Kato for his skillful operation of the accelerator during the course of this experiment.

[1]E. Merzbacher and H. W. Lewis, *Handbuch der Physik*, edited by S. Flügge (Springer, Berlin, 1958), Vol. 34, p. 166.
[2]J. D. Garcia, Phys. Rev. A 1, 280 (1970).
[3]C. H. Rutledge and R. L. Watson, At. Nucl. Data Tables 12, 195 (1973).
[4]R. L. Watson, C. W. Lewis, and J. B. Natowitz, Nucl. Phys. A 154, 561 (1970).
[5]G. A. Bissinger, A. B. Baskin, B. H. Choi, S. M. Shafroth, J. M. Howard, and A. W. Waltner, Phys. Rev. A 6, 545 (1972).
[6]S. M. Shafroth, G. A. Bissinger, and A. W. Waltner, Phys. Rev. A 7, 566 (1973).
[7]L. M. Winters, J. R. McDonald, M. D. Brown, E. L. Ellsworth, and T. Chiao, Phys. Rev. A 7, 1276 (1973).
[8]C. E. Busch, A. B. Baskin, P. H. Nettles, S. M. Shafroth, and A. W. Waltner, Phys. Rev. A 7, 1601 (1973).
[9]S. Datz, J. L. Duggan, L. C. Feldman, E. Laegsgaard, and J. U. Andersen, Phys. Rev. A 9, 192 (1974).
[10]D. H. Madison, A. B. Baskin, C. E. Busch, and S. M. Shafroth, Phys. Rev. A 9, 675 (1974).
[11]F. Abrath and T. J. Gray, Phys. Rev. A 9, 682 (1974).
[12]R. Akselsson and T. B. Johansson, Z. Phys. 266, 245 (1974).
[13]H. Tawara, K. Ishii, S. Morita, H. Kaji, C. N. Shu, and T. Shiokawa, Phys. Rev. A 9, 1617 (1974).
[14]K. Ishii, S. Morita, H. Tawara, H. Kaji, and T. Shiokawa, Phys. Rev. A 10, 774 (1974).
[15]N. Stolterfoht, D. Schneider, and P. Ziem, Phys. Rev. A 10, 81 (1974).
[16]W. Bambynek, B. Crasemann, R. W. Fink, H. U. Freund, H. Mark, C. D. Swift, R. E. Price, and P. Venugopala Rao, Rev. Mod. Phys. 44, 716 (1972).
[17]E. J. McGuire, Phys. Rev. A 3, 587 (1971).
[18]H. Tawara, M. Hyakutake, Y. Wakuta, and S. Sonoda, Genshikaku Kenkyu 12, 13 (1968).
[19]J. H. Scofield, Phys. Rev. 179, 9 (1969).
[20]B. H. Choi, E. Merzbacher, and G. S. Khandelwal, At. Data 5, 291 (1973).
[21]J. S. Hansen, Phys. Rev. A 8, 822 (1973).
[22]A. Fahlenius and P. Jauho, Ann. Acad. Sci. Fenn. A, No. 367 (1971).
[23]E. M. Bernstein and H. W. Lewis, Phys. Rev. 95, 83 (1954).
[24]D. A. Close, R. C. Bearse, J. J. Malanify, and C. J. Umberger, Phys. Rev. A 8, 1873 (1973).
[25]R. K. Wyrick and T. A. Cahill, Phys. Rev. A 8, 2288 (1973).
[26]D. W. Nix, J. C. McGeorge, and R. W. Fink, Phys. Lett. 46A, 205 (1973).
[27]P. Venugopala Rao, J. M. Palms, and R. E. Wood, Phys. Rev. A 3, 1568 (1971).
[28]J. H. McCrary, L. V. Singman, L. H. Ziegler, L. D. Looney, C. M. Edmonds, and C. E. Harris, Phys. Rev. A 5, 1587 (1972).
[29]B. H. Choi, Phys. Rev. A 4, 1002 (1971).
[30]W. Brandt and G. Lapicki, Phys. Rev. A 10, 474 (1974).
[31]J. D. Garcia, E. Gerjuoy, and J. E. Welker, Phys. Rev. 165, 72 (1968).
[32]J. H. McGuire and P. Richard, Phys. Rev. A 8, 1374 (1973).
[33]G. Basbas, W. Brandt, R. Laubert, A. Ratkowski, and A. Schwarzchild, Phys. Rev. Lett. 27, 171 (1971).
[34]C. W. Lewis, R. L. Watson, and J. B. Natowitz, Phys. Rev. A 5, 1773 (1972).
[35]K. Ishii, S. Morita, H. Tawara, H. Kaji, and T. Shiokawa, Phys. Rev. A 11, 119 (1975).
[36]K. G. Harrison, H. Tawara, and F. J. de Heer, Physica 66, 16 (1973); G. D. Goolen, J. H. McGuire, and M. H. Mittleman, Phys. Rev. A 7, 1800 (1973).
[37]J. H. McGuire and M. H. Mittlemann, Phys. Rev. A 5, 1971 (1972).
[38]T. L. Hardt and R. L. Watson, Phys. Rev. A 7, 1917 (1973).
[39]G. Pepper, R. P. Lear, T. J. Gray, and R. P. Chaturvedi (private communication).